FULL PAPER
Anatomy

Expressions of vascular endothelial growth factor receptors, Flk1 and Flt1, in rat skin mast cells during development

**Miki KOH[1), Syunya NOGUCHI[1), Mami ARAKI[1), Hirotada OTSUKA[1),
Makoto YOKOSUKA[2) and Satoshi SOETA[1)***

[1)Laboratory of Veterinary Anatomy, Faculty of Veterinary Science, Nippon Veterinary and Life Science University, 1-7-1, Kyonan-cho, Musashino-shi, Tokyo 180-8602 Japan
[2)Laboratory of Comparative and Behavioral Medicine, Faculty of Veterinary Science, Nippon Veterinary and Life Science University, 1-7-1, Kyonan-cho, Musashino-shi, Tokyo 180-8602 Japan

ABSTRACT. Vascular endothelial growth factor-A (VEGF-A) is a principal regulator of hematopoiesis as well as angiogenesis. However, the functions of VEGF-A and its receptors (VEGFRs) in the differentiation of mast cells (MCs) in the skin remain unclear. The aim of this study was to determine the expression patterns of two VEGFRs (Flk1 and Flt1) in the skin MCs during development and maturation in rats. From the 17th days of embryonic development (E17) to 1 day after birth (Day 1), most of skin MCs were immature cells containing predominant alcian blue (AB)$^+$ rather than safranin O (SO)$^+$ granules (AB>SO MCs). AB>SO MC proportions gradually decreased, while mature AB<SO MC proportions increased from Day 7 to 28. Flk1$^+$ MC proportions increased from E20 and reached to approximately 90% from Day 1 to 21, thereafter decreased to about 10% at Day 60 and 90. Flk1$^+$ MC proportions changed almost in parallel with the numbers of MCs and Ki67$^+$ MC proportions from E17 to Day 90. The proportions of MCs with both nuclear and cytoplasmic Flt1-immunoreactivity were markedly increased at Day 28, when the proportions of nuclear Flk1$^+$, Ki67$^+$, and AB>SO MCs had significantly decreased, and AB<SO MC proportions significantly increased. Considering that the main function of Flt1 is suppression of Flk1 effects, our results indicated that cross-talk between Flk1 and Flt1 regulates the proliferation and maturation of the skin MCs during late embryonic and neonatal development in rats.

KEY WORDS: Flk1, Flt1, mast cell, rat, vascular endothelial growth factor receptor

Mast cells (MCs) are common elements of connective tissue in mammals and play a central role in allergic reactions [44]. It is believed that MCs arise from multipotent hematopoietic progenitors in bone marrow and migrate to the peripheral tissues during embryonic development [40, 41]. Normally, MCs do not mature before leaving the bone marrow and complete their development and maturation within the peripheral tissues [40, 41]. In rats, the differentiation of MCs is observed histologically in the peripheral tissues, such as the mesentery, respiratory tract, and skin [5, 6, 13, 38, 61]. Skin MCs are first detected between fetal days 14–16 and differentiate to mature MCs during the fetal and neonatal stages in rodents [5, 6, 13, 37, 38]. A current study using a new fate-mapping model suggested that skin MCs in postnatal and adult mice predominantly arise from long-lived, tissue-resident MC precursors generated in the yolk-sac or differentiated from hematopoietic stem cells in the aorta-gonad-mesonephros (AGM) region that migrated to skin during embryogenesis [32]. Development of MCs is regulated by many growth factors and cytokines such as stem cell factor (SCF), IL-3, and IL-4 [62]. In skin, SCF produced by dermal fibroblasts and keratinocytes plays a crucial role in the proliferation and differentiation of MCs [59]. However, the regulatory mechanism of MC differentiation in the skin remains to be elucidated.

Vascular endothelial growth factor-A (VEGF-A) is a key angiogenic factor mainly expressed by endothelial cells and regulates endothelial cell proliferation, angiogenesis and vascular permeability via its receptors, including VEGFR1 (Flt1) and VEGFR2 (Flk1) [24, 49]. VEGF-A is also a principal regulator of hematopoiesis [11, 25]. VEGF-A inhibits total colony formation from less mature progenitor cells and promotes the formation of myeloid, mixed and erythroid colonies from lineage-committed progenitors [18, 29]. Furthermore, VEGF-A up-regulates cell survival and/or proliferation in human hematopoietic stem cells (HSC) via Flk1 [17, 33, 53], while VEGF-A/Flt1 signaling promotes cell cycling and differentiation of HSC [33, 34].

Detoraki *et al.* [16] reported on the expression of Flt1 and Flk1 in human lung MCs with VEGF-A, which promotes chemotaxis of these cells via activation of both Flt1 and Flk1. Expression of these proteins is also detected in canine MC tumors [51] and MCs

infiltrating in oral squamous cell carcinomas [12]. However, the functions of VEGF-A and VEGFRs in the differentiation of skin MCs remains to be elucidated. More histological data on VEGFRs expression in MCs are necessary in order to understand the functions of VEGF-A and VEGFRs in skin MCs during the development and maturation periods.

Therefore, in the present study, we determined the expression patterns of Flt1 and Flk1 in the skin MCs of fetal and neonatal rats. In addition, we performed sequential alcian blue (AB) and saflanin O (SO) staining as well as immunohistochemical analysis for two lineage-specific markers, c-Kit and mast cell protease 6 (MCP6, tryptase beta 2), to assess the differentiation and maturation of the MCs. We also evaluated the proliferative ability of the MCs by Ki67 immunohistochemical analysis.

MATERIALS AND METHODS

Animals

All animal handling and experimental protocols were approved by the Nippon Veterinary and Life Science University Institutional Animal Care and Use Committee. Thirty fetal Wistar rats at 15 to 20 days of embryonic development (E15 to E20, five rats at each day) and 28 neonatal and young male Wistar rats at 1, 7, 14, 21, 28, 60 and 90 days after birth (Day 1 to 90, 4 rats at each day) were used. All animals were purchased from Tokyo Laboratory Animals Science (Tokyo, Japan). To collect embryos, pregnant rats were decapitated under deep anesthesia with pentobarbital (50 mg/kg by intraperitoneal injection). The collected embryos were cut transversely and fixed in 4% paraformaldehyde in 0.1 M phosphate buffer (PB, pH 7.4) for 24 hr at 4°C. Neonatal rats were also sacrificed by deep anesthesia with pentobarbital (50 mg/kg by intraperitoneal injection), followed by decapitation. Skin tissues of the neck and the back were removed and fixed in 4% paraformaldehyde in 0.1 M PB, pH 7.4 for 24 hr at 4°C. The specimens were embedded in paraffin according to standard procedures, and cut into 3–4 μm-thick for hematoxylin and eosin (HE), alcian blue (AB) staining, and sequential AB and safranin O (AB-SO) staining or processed for immunohistochemistry (IHC).

AB staining and sequential AB-SO staining

To identify MCs in the skin, AB staining was performed according to a standard procedure [56]. Cells containing AB$^+$ cytoplasmic granules were identified as MCs and counted in 10 fields of 1 mm^2 areas. The numbers of these cells are described as means of 4 or 5 animals at each stage.

In AB-SO staining of connective type MCs including skin MCs, immature MCs contain cytoplasmic granules stained with only AB. The maturation of MCs is accompanied with increase of SO$^+$ cytoplasmic granules [5, 31]. To evaluate the differentiation and maturation of MCs in the skin, sequential AB-SO staining was conducted as previously described by Gaytan *et al* [31]. Briefly, deparaffinized sections were stained with 1% AB in 3% acetic acid (pH 2.2) for 30 min, and then with 0.5% SO in 0.125 N HC1 (pH 1.5) for 15 min. AB$^+$ and/or SO$^+$ MCs were categorized into 3 groups according to the methods previously described [13, 21, 31] with slight modifications: (1) AB>SO MCs representing immature MCs with predominant AB$^+$ cytoplasmic granules stained in blue and dark blue; (2) AB=SO MCs almost equally containing both AB$^+$ and SO$^+$ cytoplasmic granules; (3) AB<SO MCs representing mature MCs with predominant SO$^+$ cytoplasmic granules stained in dark red and brick red. Each number of AB>SO, AB=SO, and AB<SO MCs was counted in 100 AB$^+$ and /or SO$^+$ MCs in 3–5 sections from each animals and described as means of 4–5 animals at each stage.

IHC

According to the information provided by the manufacturers, all antibodies used in this study reacted to rat antigens. Deparaffinized sections were treated with methanol containing 0.3% H$_2$O$_2$ for 30 min to block endogenous peroxidase activity. After being washed in 0.01 M phosphate-buffered saline (PBS, pH 7.4), the sections were incubated in 0.01 M citrate buffer (pH 6.0) at 67°C for 60 min (for Flk1, Flt1, c-Kit, and MCP6) [42] or heated in a microwave at 500 W for 5 min three times (for Ki67). After treatment with Block Ace (Snow Brand Milk Products Co., Tokyo, Japan), the sections were incubated with various primary antibodies (Table 1) overnight at 4°C. After washing in PBS, the sections were incubated with appropriate horseradish peroxidase (HRP)-conjugated secondary antibodies (Table 1). The reaction products were visualized using DAB solution (EnVision+; DAKO, Glostrup, Denmark). Finally, the sections were counterstained with hematoxylin or AB. The numbers of immunoreactive AB$^+$ MCs were counted in 100 AB$^+$ MCs in 3–5 sections from each animal and described as means of 4–5 animals at each stage.

Double-labeling IHC

To confirm that Flk1- and Flt1-immunoreactivies were localized in MCs, double-labeling IHC was performed using two MC

Table 1. Primary antibodies used in the experiment

Antibody	Host species	Dilution	Supplier	Article No.
Anti-Flk1	Mouse, monoclonal	1:100	Santa Cruz, Dallas, TX., USA	sc-393163
Anti-Flt1	Rabbit, polyclonal	1:100	Santa Cruz, Dallas, TX., USA	sc-316
Anti-c-Kit	Rabbit, polyclonal	1:100	Agilent, Santa Clara, CA., USA	A4502
Anti-MCP6	Mouse, monoclonal	1:500 (1:100)[a]	Santa Cruz, Dallas, TX., USA	sc-59587
Anti-Ki67	Rabbit, polyclonal	1:500	ABCAM, Cambridge, UK	ab15580

a) For detection using fluor-labeled secondary antibody.

marker antibodies, anti-c-Kit antibody (raised in rabbit) for ant-Flk1 antibody (raised in mouse) and ant-MCP6 antibody (raised in mouse) for anti-Flt1 antibody (raised in rabbit). The combinations of anti-Flk1 and anti-c-Kit antibodies, and anti-Flt1 and anti-MCP6 antibodies were used at appropriate dilution as described in Table 1. To evaluate the localization of Ki67-immunoreactivity in Flk1$^+$ MCs and co-expression of Flk1 and Flt1 in MCs, double-labeling IHCs were conducted using cocktails of anti-Flk1 mouse monoclonal and anti-Ki67 rabbit polyclonal antibodies, and anti-Flk1 mouse monoclonal and anti-Flt1 rabbit polyclonal antibodies at appropriate dilution as described in Table 1. The antigen-antibody reactivities were detected using a cocktail of Alexa Fluor 488-conjugated anti-mouse IgG goat antibody (Invitrogen, Carlsbad, CA., USA; 1:250, for Flk1 and MCP6) and Alexa Fluor 568-conjugated anti-rabbit IgG donkey antibody (Invitrogen; 1:250, for c-Kit, Ki67 and Flt1). In the double-labeling IHC for Ki67 and Flk1, and Flk1 and Flt1, the sections were counterstained with AB to confirm the presence of immunoreaction in MCs. The sections were examined using the DP2-BSW software (Olympus, Tokyo, Japan) or BZ-X 170 Viewer and BZ-X Analyzer (KEYENCE, Osaka, Japan). In several sections, red or blue fluorescence was converted to magenta using software BZ-X Analyzer (KEYENCE) to demonstrate the nuclear localization of immunoreactivities more clearly.

Statistical analysis

The results of AB staining, AB-SO staining and IHC were statistically evaluated using one-way ANOVA and Tukey's *post hoc* test. Differences were considered to be statistically significant at $P<0.05$.

RESULTS

Maturation and proliferation of skin MCs

In AB staining, MCs were first detectable in the skin at E16 as round cells containing AB$^+$ cytoplasmic granules. As shown in Fig. 1, the numbers of AB$^+$ MCs were gradually increased from E19 and showed significantly higher levels from E20 to Day 21, followed by significantly lower levels from Day 28 to 90 ($P<0.001$, Fig. 1D). In AB-SO staining, all MCs were classified as AB>SO MCs from E16 to Day 1 (Fig. 1A and 1E). The proportion of AB>SO MCs were decreased from Day 7 and showed significantly lower levels after Day 21 ($P<0.001$, Fig. 1E). Notably, AB>SO MCs were almost disappeared from Day 28 to 90 (Fig. 1E). A small numbers of AB=SO MCs first appeared at Day 7, and their proportions significantly increased to about 50% of MCs at Day 14 and 21 ($P<0.001$, Fig. 1B and 1E). However, the proportions of these cells gradually decreased from Day 28 and showed significantly lower levels at Day 90 ($P<0.001$, Fig. 1E). SO>AB MCs were clearly identified at Day 7; thereafter, the proportions of these cells significantly increased to approximately 90% of MCs after Day 28 ($P<0.001$, Fig. 1E). Skin MCs predominantly consisted of SO>AB MCs at Day 60 and 90 (Fig. 1C and 1E). The presence of AB$^+$ granules was confirmed in all MCs, including AB>SO, AB=SO, and AB<SO MCs by observation of AB staining before applying SO in AB-SO staining from E16 to Day 90.
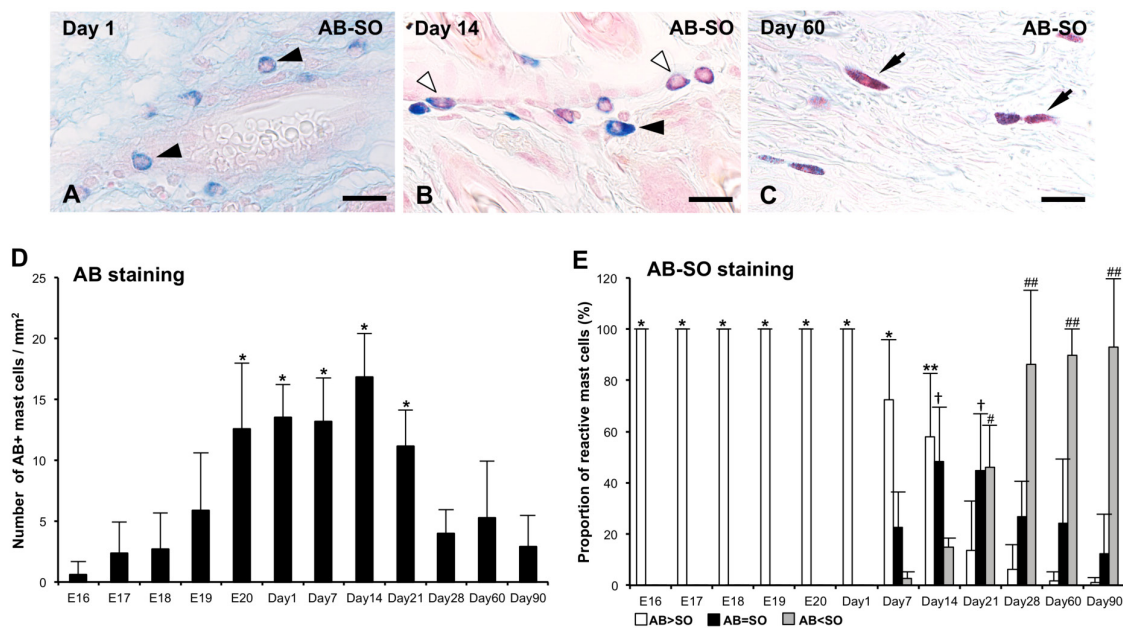

Fig. 1. Alcian blue (AB) -safranin O (SO) staining of skin mast cells (MCs) at 1 day after birth (Day 1) (A), Days 14 (B), and 60 (C). (A) Only AB>SO MCs (black arrowheads) are detected at Day 1. (B) Both AB>SO and AB=SO MCs (white arrowheads) are identified at Day 14. (C) AB<SO MCs (black arrowheads) constitute most of skin MCs at Day 60. Bar=20 μm (A–C). (D) Numbers of MCs identified as AB$^+$ cells per 1 mm^2 of the skin from 16 days of embryonic development (E16) to Day 90. Data are presented as means ± SD. *$P<0.001$ vs E16–18 and Days 28–90. (E) The proportions of AB>SO, AB=SO, and AB<SO MCs from E16 to Days 90 are presented as means ± SD. *$P<0.001$ vs Days 7–21; **$P<0.001$ vs Days 21–90; †$P<0.001$ vs Days 1 and 90; #$P<0.001$ vs Days 7; ##$P<0.001$ vs Days 7 and 14.
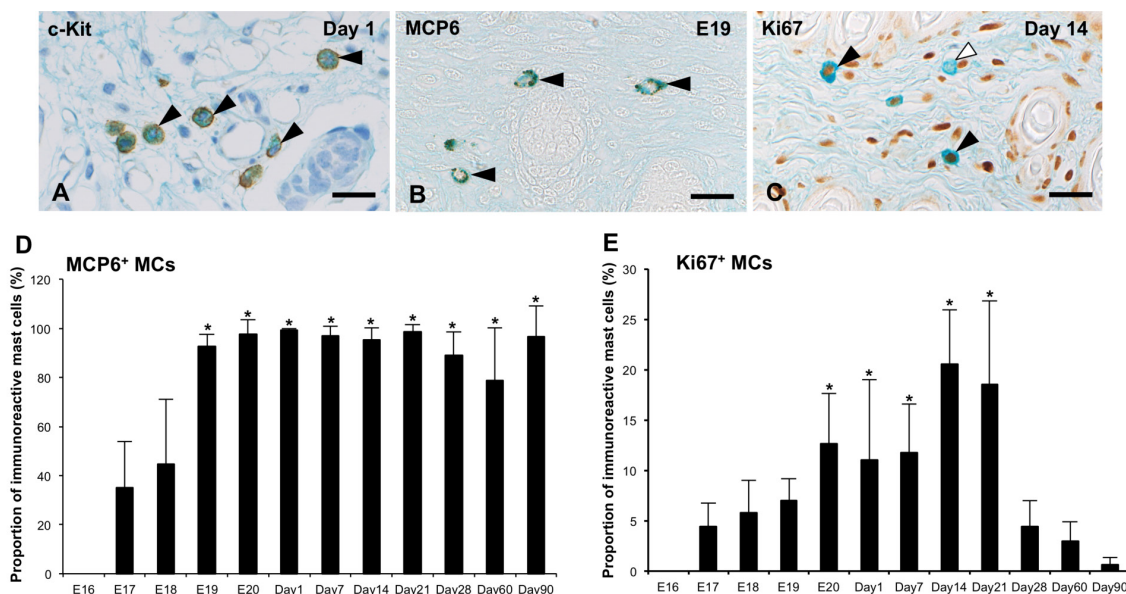
Fig. 2. (A) c-Kit-immunoreactivity (black arrowheads) is detected in the cell membrane and/or cytoplasm of all alcian blue (AB) [+] MCs at 1 day after birth (Day 1). (B) MCP6-immunoreactivity (black arrowheads) is detected in the cytoplasm of all AB[+] MCs at 19 days of embryonic development (E19). (C) Ki67-immunoreactivity (black arrowheads) is shown in the nucleus of several MCs at Day 14. White arrowheads denote Ki67-immunonegative MCs. Bar=20 μm (A–C). (D) The proportion of MCP6^{+} MCs from E16 to Day 90 are presented as means ± SD. *$P<0.001$ vs E17 and 18. (E) The proportion of Ki67^{+} MCs from E16 to Day 90 are presented as means ± SD. *$P<0.001$ vs E17 and Days 28–90.

c-Kit-immunoreactivity was detected in the cell membrane and/or cytoplasm in all AB[+] MCs in all samples from E16 to Day 90 (Fig. 2A). However, MCP6-immunoreactivity was first identified in a small number of AB[+] MCs at E17 (Fig. 2D). The number of MCP6^{+}/AB[+] MCs increased from E18, and most of AB[+] MCs showed MCP6-immunoreactivity from E19 to Day 90 (Fig. 2B and 2D).

Ki67-immunoreactivity was detected in the nuclei of AB[+] MCs from E17 to Day 90 (Fig. 2E). The Ki67^{+} MCs were detected in approximately 5–10% of AB[+] MCs from E17 to Day 7; thereafter, the proportions of these cells significantly increased to approximately 20% at Days 14 and 21 ($P<0.001$, Fig. 2C and 2E). However, the proportions of Ki67^{+} MCs significantly decreased at Day 28 ($P<0.001$), and the immunoreactive MCs had almost disappeared by Days 60 and 90 (Fig. 2E).

Flk1- and Flt1-IHC

Flk1-immunmoreactivity was found in the nuclei and/or cytoplasm of AB[+] MCs from E17 to Day 90 (Fig. 3). From E17 to 19, approximately 18–26% of AB[+] MCs showed Flk1-immunoreactivity only in the cytoplasm (cytFlk1, Fig. 3I). The proportion of cytFlk1[+] MCs was found to have significantly increased from E19 to E20 ($P<0.001$), and approximately 70% of AB[+] MCs showed cytFlk1-immunoreactivity from Day 1 to 21 (Fig. 3A and 3I). However, the proportion of these MCs decreased after Day 28, and subsequently showed significantly lower levels at Day 60 and 90 ($P<0.001$, Fig. 3I). Flk1-immunoreactivity in the nuclei as well as the cytoplasm (nuc/cytFlk1) was identified in small numbers of AB[+] MCs at E17 and 18 (Fig. 3B and 3I). The nuc/cytFlk1[+] MCs constituted 10–30% of AB[+] MCs from E19 to Day 21 (Fig. 3B and 3I), and thereafter the proportion of these cells significantly decreased to approximately 2% of AB[+] MCs after Day 28 ($P<0.001$, Fig. 3C and 3I). Double-labeling IHC confirmed that Flk1-immunoreactivity was localized in the MCs identified by c-Kit immunoreactivity from E17 to Day 90 (Fig. 3D–G). In addition, nuclear and cytoplasmic localization of Flk1-immunoreactivity in c-Kit[+] MCs was confirmed by double-labeling IHC with DAPI nuclear staining from Days 1 to 21 (Fig. 3D–G). Double-labeling IHC for Ki67 and Flk1 revealed that all Ki67-immunoreactive AB[+] MCs showed cyt or nuc/cytFlk1-immunoreactivity from E17 to Day 28 (Fig. 4).

Flt1-immunoreactivity was also detected in the nuclei and/or the cytoplasm of AB[+] MCs from E19 to Day 90 (Fig. 5). Flt1-immunoreactivity only in the cytoplasm (cytFlt1) was detected in a small number of AB[+] MCs at E19 (Fig. 5M). The proportion of the cytFlt1[+] MCs was found to significantly increase from E19 to E20 ($P<0.001$, Fig. 5M); thereafter, these MCs constituted approximately 60% of AB[+] MCs from Day 1 to 7 (Fig. 5A and 5M). However, the proportions of cytFlt1[+] MCs was found to decrease from Day 14 and showed significantly lower levels after Day 28 ($P<0.001$, Fig. 5M). Both nuclear and cytoplasmic localization of Flt1-immunoreactivity (nuc/cytFlt1) was detected in a small number of AB[+] MCs from E19 to Day 14 (Fig. 5B and 5M). The proportion of these MCs was found to increase after Day 14 and showed significantly higher levels at Day 21 and 28. However, the proportion significantly decreased after Day 60 ($P<0.001$, Fig. 5M). Double-labeling IHC confirmed that the MCs identified by MCP6-immunoreactivity showed Flt1-immunoreactivity from E19 to Day 90 (Fig. 5C–K). In addition, the presence of cytoFlt1[+]MCP6^{+} MCs (Fig. 5C–E) and nuc/cytoFlt1[+]MCP6^{+} MCs (Fig. 5F–K) was clearly identified from Days 1 to 28 by the double-labeling IHC with DAPI staining.

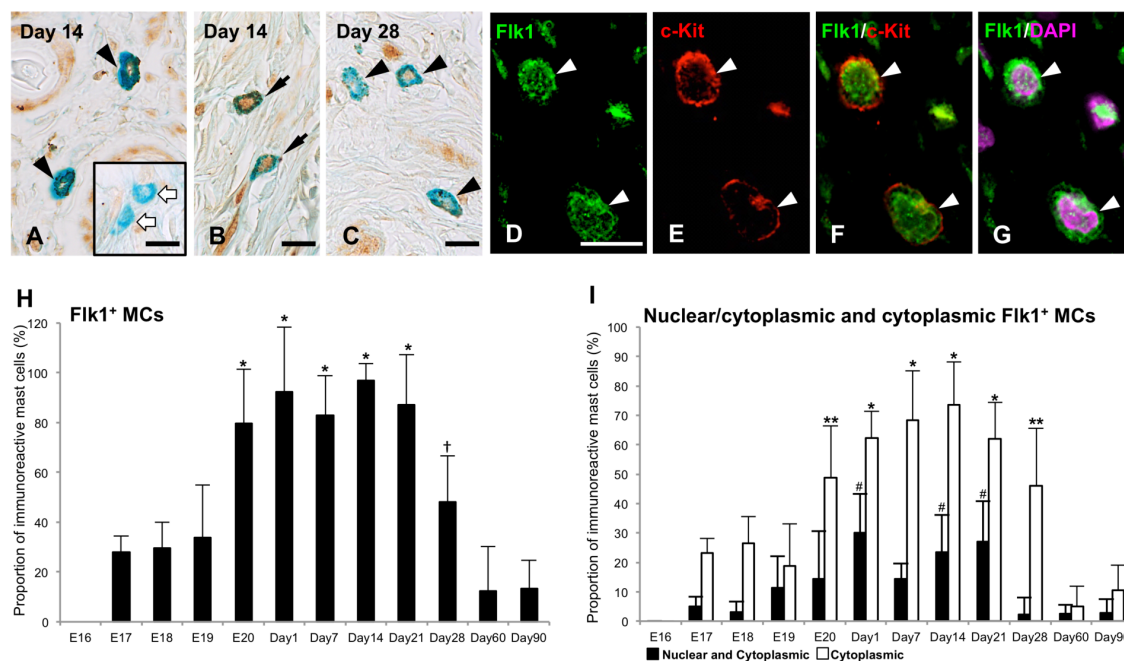Double-labeling IHC for Flk1 and Flt1 revealed the colocalization of both Flk1- and Flt1-immunoreactivities in most of AB[+]

Fig. 3. Flk1-immunohistochemistry (IHC) in skin mast cells (MCs) at 14 days after birth (Day 14) (A, B and D–G) and Day 28 (C). (A and B) Flk1-immunoreactivity is detected both in the nucleus and cytoplasm (black arrows) or only in the cytoplasm (black arrowheads) of MCs at Day 14. White arrows denote Flk1-immunonegative MCs. (C) Flk1-immunoreactivity is detected only in the cytoplasm of MCs at Day 28. (D–G) Double-labeling IHC for Flk1 (green, D) and c-Kit (red, E) with DAPI (magenta) of skin MCs (white arrowheads) at Day 14. (F) Merged image of D and E confirms the presence of Flk1-immunoreactivity in c-Kit$^+$ MCs. (G) Merged image of Flk1-IHC (green, D) and DAPI (magenta) reveals the localization of Flk1-immunoreactivity both in the cytoplasm and nucleus of the c-Kit$^+$ MCs (white arrowheads). Bar=20 μm (A–G). (H) The proportions of Flk1$^+$ MCs from 16 days of embryonic development (E16) to Day 90 are presented as means ± SD. *$P<0.001$ vs E17–19 and Days 60–90; †$P<0.001$ vs Days 60–90. (I) The proportions of nuclear/cytoplasmic and cytoplasmic Flk1$^+$ MCs from E16 to Day 90 are presented as means ± SD. *$P<0.001$ vs E17–19 and Days 60–90; **$P<0.001$ vs Days 60–90; #$P<0.001$ vs E19-Day 14 and Days 28–90.
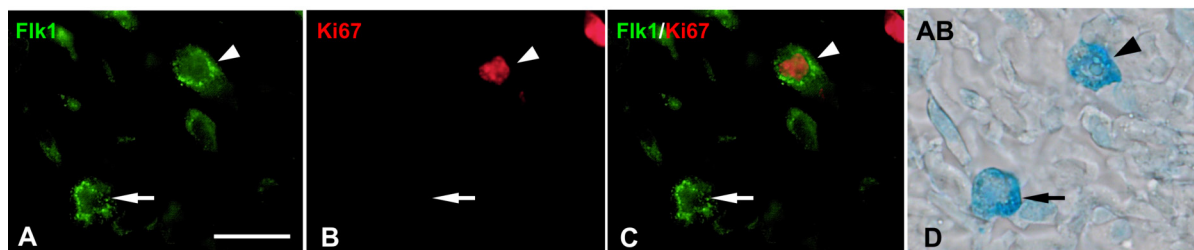

Fig. 4. Double-labeling immunohistochemistry for Flk1 (green, A) and Ki67 (red, B) in alcian blue (AB)$^+$ mast cells (MCs) (D) at 14 days after birth (A–D). (C) Merged image of A and B reveals the colocalization of cytoplasmic Flk1- and Ki67-immunoreactivities (white arrowhead). White arrows denote Flk1$^+$Ki67$^-$ MCs. Black arrowhead and arrow in D represent same cells marked by white arrowheads and arrows in A–C, respectively. Bar=20 μm.

MCs from Day 1 to 28 (Fig. 6). Flk1$^+$Flt1$^+$AB$^+$MCs consisted of nuc/cytFlt1$^+$nuc/cytFlk1$^+$ (Fig. 6A–D), nuc/cytFlt1$^+$cytFlk1$^+$ (Fig. 6A–D), cytFlt1$^+$nuc/cytFlk1$^+$ and cytFlt1$^+$cytFlk1$^+$ MCs from Days 1 to 21. At Day 28, however, Flk1$^+$Flt1$^+$AB$^+$ MCs showed only cytoplasmic Flk1, but not nuclear Flk1-immunoreactivity (Fig. 6E–H).

DISCUSSION

In this study, we demonstrated the localization of Flk1- and Flt1-immunoreactivities in skin MCs during late embryonic and neonatal development in rats. The proportions of Flk1- and Flt1-expressing MCs were especially pronounced from Day 1 to 28. However, these immunoreactivities had almost disappeared in the skin MCs at Days 60 and 90. To our knowledge, expression of Flk1 and Flt1 in normal MCs has been reported only in two studies on MCs infiltrating oral squamous cell carcinomas and in those isolated from normal lungs [12, 16]. This is the first report showing significant expression of Flk1 and Flt1 in skin MCs
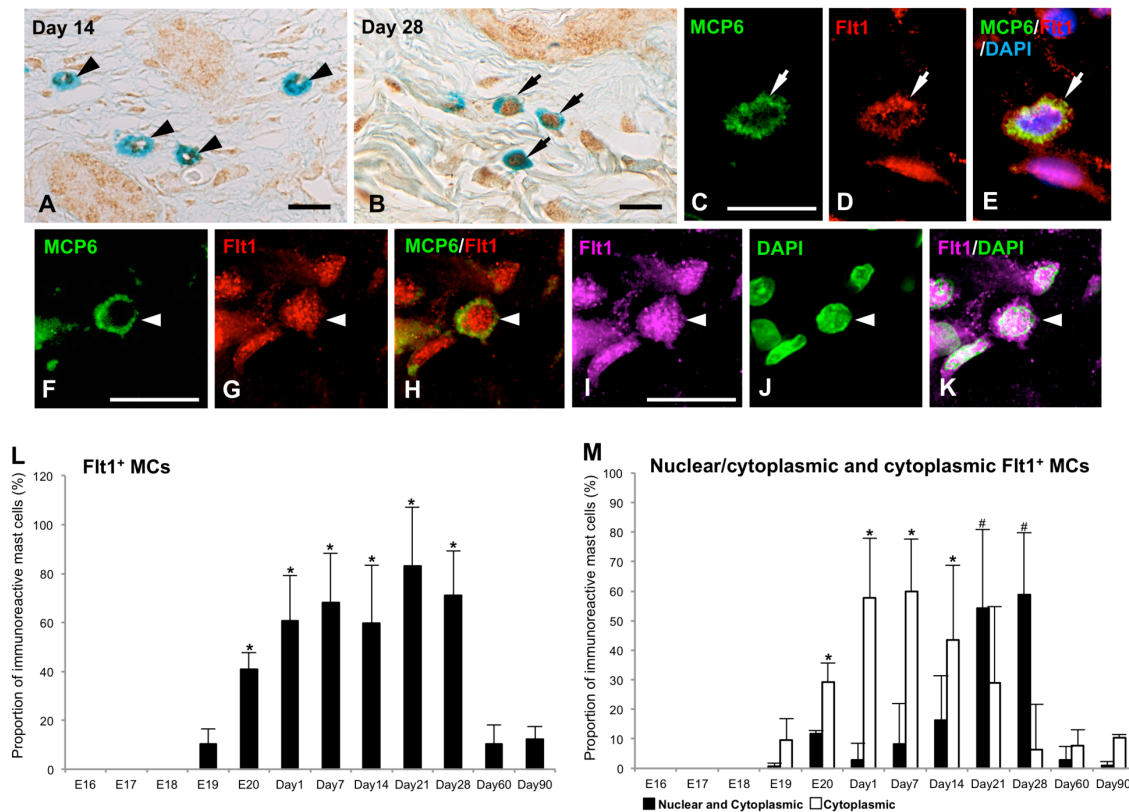
Fig. 5. Flt1-immunohistochemistry (IHC) in skin mast cells (MCs) at 14 days after birth (Day 14) (A) and Day 28 (B). (A) Flt1-immunoreactivity is detected only in the cytoplasm in most of MCs (black arrowheads) at Day 14. (B) Flt1-immunoreactivity is detected both in the nucleus and cytoplasm in most of MCs (black arrows) at Day 28. (C–E) Double-labeling IHC for MCP6 (green, C) and Flt1 (red, D) with DAPI (blue) of the skin MCs (white arrows) at Day 14. (E) Merged image of C and D confirms the localization of Flt1-immunoreactivity in the cytoplasm of MCP6^{+} MCs (yellow). (F–K) Double-labeling IHC for MCP6 (green, F) and Flt1 (red, G; magenta, I) with DAPI (green, J) of the skin MCs (white arrowheads) at Day 28. (H and K) Merged images of F and G (H), and I and J (K) confirm the localization of Flt1-immunoreactivity both in the cytoplasm (yellow, H; magenta, K) and nucleus (red, H; white, K) of MCP6^{+} MCs. Bar=20 μm (A–K). (L) The proportions of Flt1^{+} MCs from 16 days of embryonic development (E16) to Day 90 are presented as means ± SD. *$P<0.001$ vs E19 and Days 60-90. (M) The proportions of nuclear/cytoplasmic and cytoplasmic Flt[+] MCs from E16 to Day 90 are presented as means ± SD. *$P<0.001$ vs E19 and Days 28–90; #$P<0.001$ vs E19-Day 7 and Days 60–90.
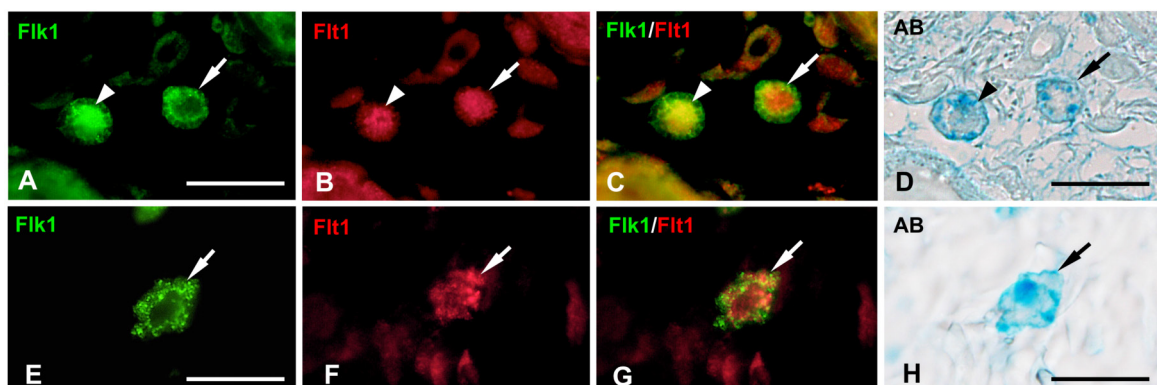

Fig. 6. Double-labeling immunohistochemistry (IHC) for Flk1 (green, A and E) and Flt1 (red, B and F) in alcian blue (AB)[+] mast cells (MCs) (D and H) at 21 days after birth (Day 21) (A–D) and 28 (E–H). (C) Merged image of A and B reveals the colocalization of nuclear/cytoplasmic Flk1- and nuclear/cytoplasmic Flt-immunoreactivities (white arrowheads), or cytoplasmic Flk1- and nuclear/cytoplasmic Flt1-immunoreactivities (white arrows) in most of MCs at Day 21. (G) Merged image of E and F confirms the presence of only MCs showing colocalization of cytoplasmic Flk1- and nuclear/cytoplasmic Flt1-immunoreactivities (white arrows) at Day 28. (D) Black arrowheads and arrows represent same cells marked by white arrowheads and arrows in A–C, respectively. (H) Black arrow represents a same cell marked by white arrow in E–G. Bar=20 μm.

during development and maturation. Several studies revealed that MC lineages differentiate to mature MCs after recruitment to the skin during late embryonic development. Immature MCs containing only AB^+ cytoplasmic granules increase SO^+ granules with maturation and consequently differentiate to mature MCs with predominant SO^+ cytoplasmic granules in the skin [13]. The AB-SO staining results revealed that the skin MCs consisted of only AB>SO immature MCs from E16 to Day 1; thereafter, AB<SO mature MCs appeared at Day 7 and increased to a maximum level at Day 28. These findings indicate that differentiation to mature MCs is especially up-regulated from Day 7 to 28. At Day 60 and 90, immature AB>SO MCs almost disappeared, and mature AB<SO MCs constituted a major population of the skin MCs, implying that the maturation process of MCs was reduced in the skin of young adult rats. Thus, our findings suggested that Flk1 and Flt1 are predominantly expressed in skin MCs during the maturation process and play a crucial role in the regulation of these MCs.

Flk1 is a key regulator of angiogenesis, acting through the promotion of proliferation and survival of the endothelial cells [23, 35, 47, 57]. In various types of hematopoietic cells, including acute myeloid leukemia, B-cell chronic lymphocytic leukemia, and HSCs, VEGF-A/Flk1 signaling enhances cell proliferation and survival [20, 36]. In this study, the proportion of $Flk1^+$ MCs changed in almost parallel with the number of AB^+ MCs from E17 to Day 90. Furthermore, the MCs showed significantly higher levels of $Flk1^+$ MC proportions from E20 to Day 21, accompanied with significantly higher levels of $Ki67^+$ MC proportions. In addition, all Ki67-immunoreactive MCs showed Flk1 expression. These findings indicated that VEGF-A/Flk1 signaling contributes to upregulation of MC proliferation in the skin. Detoraki et al. [16] demonstrated that VEGF-A promoted chemotactic migration of MCs, especially via Flk1 using normal lung MCs. Therefore, the increase of MCs observed in this study may have been caused by enhanced migration of MCs due to VEGF-A/Flk1 signaling as well as proliferation of MCs. However, skin MCs are predominantly differentiated from long-lived, skin-resident MC precursors, and do not migrate from bone marrow in mice [32]. In addition, to the best of our knowledge, there is no report indicating the migration of skin MCs from other sites during embryonic or postnatal development. Thus, further investigation will be required to determine the contribution of VEGF-A and Flk1 to the migration of skin MCs during development.

In this study, the skin MCs showed both cytoplasmic and nuclear localization of Flk1-immunoreactivity. Unlike other related growth factor receptors, a significant proportion of Flk1 is held in an endosomal storage pool within the cytoplasm of vascular endothelial cells [8, 9, 30]. The cytoplasmic Flk1 level is increased by VEGF-A stimulation, and Flk1 is subsequently transported to the nucleus in association with endothelial nitric oxide synthase or under shear stress [20, 22, 54]. In vascular endothelial cells and acute myeloid leukemia cell lines, VEGF/Flk1 signaling induces nuclear translocation of Flk1, resulting in up-regulation of cell proliferation [27]. In addition, constitutive nuclear localization of Flk1 is found in several types of tumor cells showing proliferative activity [4, 19, 26, 55, 63]. Domingues et al. [19] concluded that nuclear Flk1 up-regulated its own transcription by binding to its own promoter dependent on Flk1 activation by VEGF-A. Thus, nuclear Flk1 may amplify the proliferative effect of Flk1 by upregulating its expression in the skin MCs.

In endothelial cells expressing both Flt1 and Flk1, the main function of Flt1 is the modulation of the angiogenic effects of VEGF-A via Flk1 [3, 10]. Membrane-bound Flt1 homomeric receptor down-regulates Flk1-mediated cell proliferation [2, 7, 50, 64], although it is poorly tyrosine-phosphorylated by VEGF-A stimulation [49, 60]. In addition, soluble Flt1 generated by alternative splicing acts as a decoy receptor and suppresses VEGF-A/Flk1 signaling by binding VEGF-A with strong affinity [28, 48, 52]. Both Flt1 isoforms also suppress Flk1 signaling by formation of heterodimers with Flk1 [14, 36, 39]. The opposite effects of Flk1 and Flt1 have also been demonstrated in hematopoietic lineages. Huang et al. revealed that Flt1 upregulated differentiation from pro-B cells to pre-B-cells, while Flk1 suppressed this process [36]. In human HSCs, VEGF-A/Flt1 signaling promotes cell cycling and differentiation [33, 34], whereas Flk1 upregulates cell survival and/or proliferation by VEGF-A stimulation [17, 33, 53]. Therefore, our results showing expression of both Flt1 and Flk1 in MCs indicate that cross-talk between these two VEGFRs regulates the MCs during maturation in the skin.

Interestingly, we found that the number of MCs with nuclear Flt1 increased from Day 14 to 28. Membrane-bound Flt1 is commonly present in the cell membrane and cytoplasmic compartments [8, 9, 15, 43, 45, 46]. However, it is also detected within nuclei in several normal tissues and neoplastic cells [1, 8, 9, 43, 58]. The nuclear Flt1 has been suggested to function as a transcription factor, similar to nuclear Flk1 [43, 58], although a detailed understanding of nuclear Flt1 functions remains to be elucidated. Therefore, nuclear Flt1 may promote expression of Flt1 in the skin MCs from Day 14 to 28. Lee et al. [43] revealed that VEGF-A stimulation induced intracellular trafficking and nuclear localization of Flt1, which was suggested to be involved in cell survival and proliferation by VEGF-A/Flt1 intracrine signaling in human breast carcinoma cells expressing only Flt1, but not Flk1 [43]. However, in endothelial cells expressing both Flt1 and Flk1, VEGF-A stimulates an increase of Flk1 and decrease of Flt1 in the nucleus, resulting in up-regulation of angiogenesis [10]. Cai et al. demonstrated that the nuclear translocation of Flt1 was promoted by pigment epithelium-derived factor, one of Flt1 ligands that inhibits angiogenesis induced by VEGF-A/Flk1 signaling [9, 10]. Furthermore, the ratio of Flt1 to Flk1 in the nucleus is a critical determinant in angiogenesis [10]. These previous results imply that Flt1 also suppresses Flk1 function in the nucleus. Our results revealed that MCs showing nuclear Flt1 increased to a maximum level, and MCs with nuclear Flk1 almost disappeared at Day 28, when $Ki67^+$ MCs drastically decreased and AB<SO MCs approached a maximum level. These results lead to the possibility that increase in the nuclear Flt1: Flk1 ratio may result in down-regulation of immature MC proliferation and induction of terminal maturation by suppressing the effects of nuclear Flk1 on the MCs. Further quantitative evaluations of nuclear Flt1 and Flk1 in the MCs are needed to confirm this hypothesis. However, our results presented here would contribute to the further studies on the functions of VEGF/VEGFRs signaling in the differentiation of skin MCs.

REFERENCES

1. Andersson, M. K., Göransson, M., Olofsson, A., Andersson, C. and Åman, P. 2010. Nuclear expression of FLT1 and its ligand PGF in FUS-DDIT3 carrying myxoid liposarcomas suggests the existence of an intracrine signaling loop. *BMC Cancer* **10**: 249. [Medline] [CrossRef]
2. Ahmed, A., Dunk, C., Kniss, D. and Wilkes, M. 1997. Role of VEGF receptor-1 (Flt-1) in mediating calcium-dependent nitric oxide release and limiting DNA synthesis in human trophoblast cells. *Lab. Invest.* **76**: 779–791. [Medline]
3. Bahramsoltani, M., De Spiegelaere, W., Janczyk, P., Hiebl, B., Cornillie, P. and Plendl, J. 2010. Quantitation of angiogenesis in vitro induced by VEGF-A and FGF-2 in two different human endothelial cultures-an all-in-one assay. *Clin. Hemorheol. Microcirc.* **46**: 189–202. [Medline] [CrossRef]
4. Blazquez, C., Cook, N., Micklem, K., Harris, A. L., Gatter, K. C. and Pezzella, F. 2006. Phosphorylated KDR can be located in the nucleus of neoplastic cells. *Cell Res.* **16**: 93–98. [Medline] [CrossRef]
5. Burton, A. L. 1964. Histochemical studies on developing mast cells. *Anat. Rec.* **150**: 265–269. [Medline] [CrossRef]
6. Burton, A. L. 1967. Differentiation of mast cells in the subcutaneous connective tissue of rat embryos. *Tex. Rep. Biol. Med.* **25**: 240–250. [Medline]
7. Bussolati, B., Dunk, C., Grohman, M., Kontos, C. D., Mason, J. and Ahmed, A. 2001. Vascular endothelial growth factor receptor-1 modulates vascular endothelial growth factor-mediated angiogenesis via nitric oxide. *Am. J. Pathol.* **159**: 993–1008. [Medline] [CrossRef]
8. Cai, J., Jiang, W. G., Grant, M. B. and Boulton, M. 2006. Pigment epithelium-derived factor inhibits angiogenesis via regulated intracellular proteolysis of vascular endothelial growth factor receptor 1. *J. Biol. Chem.* **281**: 3604–3613. [Medline] [CrossRef]
9. Cai, J., Chen, Z., Ruan, Q., Han, S., Liu, L., Qi, X., Boye, S. L., Hauswirth, W. W., Grant, M. B. and Boulton, M. E. 2011. γ-Secretase and presenilin mediate cleavage and phosphorylation of vascular endothelial growth factor receptor-1. *J. Biol. Chem.* **286**: 42514–42523. [Medline] [CrossRef]
10. Cai, J., Qi, X., Ruan, Q., Han, S., Chen, Z., Podlaski, A., Grant, M. B. and Boulton, M. E. 2012. Non-canonical VEGF receptor signaling regulates retinal neovascularization. *Invest. Ophthalmol. Vis. Sci.* **53**: 2993.
11. Carmeliet, P., Ferreira, V., Breier, G., Pollefeyt, S., Kieckens, L., Gertsenstein, M., Fahrig, M., Vandenhoeck, A., Harpal, K., Eberhardt, C., Declercq, C., Pawling, J., Moons, L., Collen, D., Risau, W. and Nagy, A. 1996. Abnormal blood vessel development and lethality in embryos lacking a single VEGF allele. *Nature* **380**: 435–439. [Medline] [CrossRef]
12. Ciurea, R., Mărgăritescu, C., Simionescu, C., Stepan, A. and Ciurea, M. 2011. VEGF and his R1 and R2 receptors expression in mast cells of oral squamous cells carcinomas and their involvement in tumoral angiogenesis. *Rom. J. Morphol. Embryol.* **52**: 1227–1232. [Medline]
13. Combs, J. W., Lagunoff, D. and Benditt, E. P. 1965. Differentiation and proliferation of embryonic mast cells of the rat. *J. Cell Biol.* **25**: 577–592. [Medline] [CrossRef]
14. Cudmore, M. J., Hewett, P. W., Ahmad, S., Wang, K. Q., Cai, M., Al-Ani, B., Fujisawa, T., Ma, B., Sissaoui, S., Ramma, W., Miller, M. R., Newby, D. E., Gu, Y., Barleon, B., Weich, H. and Ahmed, A. 2012. The role of heterodimerization between VEGFR-1 and VEGFR-2 in the regulation of endothelial cell homeostasis. *Nat. Commun.* **3**: 972. [Medline] [CrossRef]
15. Decaussin, M., Sartelet, H., Robert, C., Moro, D., Claraz, C., Brambilla, C. and Brambilla, E. 1999. Expression of vascular endothelial growth factor (VEGF) and its two receptors (VEGF-R1-Flt1 and VEGF-R2-Flk1/KDR) in non-small cell lung carcinomas (NSCLCs): correlation with angiogenesis and survival. *J. Pathol.* **188**: 369–377. [Medline] [CrossRef]
16. Detoraki, A., Staiano, R. I., Granata, F., Giannattasio, G., Prevete, N., de Paulis, A., Ribatti, D., Genovese, A., Triggiani, M. and Marone, G. 2009. Vascular endothelial growth factors synthesized by human lung mast cells exert angiogenic effects. *J. Allergy Clin. Immunol.* **123**: 1142–1149, 1149. e1–1149.e5. [Medline] [CrossRef]
17. Dias, S., Hattori, K., Zhu, Z., Heissig, B., Choy, M., Lane, W., Wu, Y., Chadburn, A., Hyjek, E., Gill, M., Hicklin, D. J., Witte, L., Moore, M. A. and Rafii, S. 2000. Autocrine stimulation of VEGFR-2 activates human leukemic cell growth and migration. *J. Clin. Invest.* **106**: 511–521. [Medline] [CrossRef]
18. Dikov, M. M., Oyama, T., Cheng, P., Takahashi, T., Takahashi, K., Sepetavec, T., Edwards, B., Adachi, Y., Nadaf, S., Daniel, T., Gabrilovich, D. I. and Carbone, D. P. 2001. Vascular endothelial growth factor effects on nuclear factor-kappaB activation in hematopoietic progenitor cells. *Cancer Res.* **61**: 2015–2021. [Medline]
19. Domingues, I., Rino, J., Demmers, J. A., de Lanerolle, P. and Santos, S. C. 2011. VEGFR2 translocates to the nucleus to regulate its own transcription. *PLoS One* **6**: e25668. [Medline] [CrossRef]
20. Dougher, M. and Terman, B. I. 1999. Autophosphorylation of KDR in the kinase domain is required for maximal VEGF-stimulated kinase activity and receptor internalization. *Oncogene* **18**: 1619–1627. [Medline] [CrossRef]
21. el Sayed, S. O. and Dyson, M. 1993. Histochemical heterogeneity of mast cells in rat dermis. *Biotech. Histochem.* **68**: 326–332. [Medline]
22. Feng, Y., Venema, V. J., Venema, R. C., Tsai, N. and Caldwell, R. B. 1999. VEGF induces nuclear translocation of Flk-1/KDR, endothelial nitric oxide synthase, and caveolin-1 in vascular endothelial cells. *Biochem. Biophys. Res. Commun.* **256**: 192–197. [Medline] [CrossRef]
23. Ferrara, N. 2004. Vascular endothelial growth factor: basic science and clinical progress. *Endocr. Rev.* **25**: 581–611. [Medline] [CrossRef]
24. Ferrara, N., Gerber, H. P. and LeCouter, J. 2003. The biology of VEGF and its receptors. *Nat. Med.* **9**: 669–676. [Medline] [CrossRef]
25. Ferrara, N., Carver-Moore, K., Chen, H., Dowd, M., Lu, L., O'Shea, K. S., Powell-Braxton, L., Hillan, K. J. and Moore, M. W. 1996. Heterozygous embryonic lethality induced by targeted inactivation of the VEGF gene. *Nature* **380**: 439–442. [Medline] [CrossRef]
26. Fox, S. B., Turley, H., Cheale, M., Blázquez, C., Roberts, H., James, N., Cook, N., Harris, A. and Gatter, K. 2004. Phosphorylated KDR is expressed in the neoplastic and stromal elements of human renal tumours and shuttles from cell membrane to nucleus. *J. Pathol.* **202**: 313–320. [Medline] [CrossRef]
27. Fragoso, R., Elias, A. P. and Dias, S. 2007. Autocrine VEGF loops, signaling pathways, and acute leukemia regulation. *Leuk. Lymphoma* **48**: 481–488. [Medline] [CrossRef]
28. Fuh, G., Li, B., Crowley, C., Cunningham, B. and Wells, J. A. 1998. Requirements for binding and signaling of the kinase domain receptor for vascular endothelial growth factor. *J. Biol. Chem.* **273**: 11197–11204. [Medline] [CrossRef]
29. Gabrilovich, D., Ishida, T., Oyama, T., Ran, S., Kravtsov, V., Nadaf, S. and Carbone, D. P. 1998. Vascular endothelial growth factor inhibits the development of dendritic cells and dramatically affects the differentiation of multiple hematopoietic lineages in vivo. *Blood* **92**: 4150–4166. [Medline] [CrossRef]
30. Gampel, A., Moss, L., Jones, M. C., Brunton, V., Norman, J. C. and Mellor, H. 2006. VEGF regulates the mobilization of VEGFR2/KDR from an intracellular endothelial storage compartment. *Blood* **108**: 2624–2631. [Medline] [CrossRef]
31. Gaytan, F., Bellido, C., Carrera, G. and Aguilar, E. 1990. Differentiation of mast cells during postnatal development of neonatally estrogen-treated rats. *Cell Tissue Res.* **259**: 25–31. [Medline] [CrossRef]
32. Gentek, R., Ghigo, C., Hoeffel, G., Bulle, M. J., Msallam, R., Gautier, G., Launay, P., Chen, J., Ginhoux, F. and Bajénoff, M. 2018. Hemogenic

endothelial fate mapping reveals dual developmental origins of mast cells. *Immunity* **48**: 1160–1171.e5. [Medline] [CrossRef]

33. Gerber, H. P., Malik, A. K., Solar, G. P., Sherman, D., Liang, X. H., Meng, G., Hong, K., Marsters, J. C. and Ferrara, N. 2002. VEGF regulates haematopoietic stem cell survival by an internal autocrine loop mechanism. *Nature* **417**: 954–958. [Medline] [CrossRef]

34. Hattori, K., Heissig, B., Wu, Y., Dias, S., Tejada, R., Ferris, B., Hicklin, D. J., Zhu, Z., Bohlen, P., Witte, L., Hendrikx, J., Hackett, N. R., Crystal, R. G., Moore, M. A., Werb, Z., Lyden, D. and Rafii, S. 2002. Placental growth factor reconstitutes hematopoiesis by recruiting VEGFR1(+) stem cells from bone-marrow microenvironment. *Nat. Med.* **8**: 841–849. [Medline] [CrossRef]

35. Helotera, H. and Alitalo, K. 2007. The VEGF family, the inside story. *Cell* **130**: 591–592. [Medline] [CrossRef]

36. Huang, Y., Chen, X., Dikov, M. M., Novitskiy, S. V., Mosse, C. A., Yang, L. and Carbone, D. P. 2007. Distinct roles of VEGFR-1 and VEGFR-2 in the aberrant hematopoiesis associated with elevated levels of VEGF. *Blood* **110**: 624–631. [Medline] [CrossRef]

37. Jamur, M. C., Lunardi, L. O. and Vugman, I. 1997. Mast cell maturation in young rats: a histofluorescence and cytochemical study. *Acta Histochem.* **99**: 379–389. [Medline] [CrossRef]

38. Jippo, T., Mizuno, H., Xu, Z., Nomura, S., Yamamoto, M. and Kitamura, Y. 1996. Abundant expression of transcription factor GATA-2 in proliferating but not in differentiated mast cells in tissues of mice: demonstration by in situ hybridization. *Blood* **87**: 993–998. [Medline] [CrossRef]

39. Kendall, R. L., Wang, G. and Thomas, K. A. 1996. Identification of a natural soluble form of the vascular endothelial growth factor receptor, FLT-1, and its heterodimerization with KDR. *Biochem. Biophys. Res. Commun.* **226**: 324–328. [Medline] [CrossRef]

40. Kitamura, Y., Go, S. and Hatanaka, K. 1978. Decrease of mast cells in W/Wv mice and their increase by bone marrow transplantation. *Blood* **52**: 447–452. [Medline] [CrossRef]

41. Kitamura, Y., Yokoyama, M., Matsuda, H., Ohno, T. and Mori, K. J. 1981. Spleen colony-forming cell as common precursor for tissue mast cells and granulocytes. *Nature* **291**: 159–160. [Medline] [CrossRef]

42. Kohara, Y., Soeta, S., Izu, Y. and Amasaki, H. 2015. Accumulation of type VI collagen in the primary osteon of the rat femur during postnatal development. *J. Anat.* **226**: 478–488. [Medline] [CrossRef]

43. Lee, T. H., Seng, S., Sekine, M., Hinton, C., Fu, Y., Avraham, H. K. and Avraham, S. 2007. Vascular endothelial growth factor mediates intracrine survival in human breast carcinoma cells through internally expressed VEGFR1/FLT1. *PLoS Med.* **4**: e186. [Medline] [CrossRef]

44. Metcalfe, D. D., Baram, D. and Mekori, Y. A. 1997. Mast cells. *Physiol. Rev.* **77**: 1033–1079. [Medline] [CrossRef]

45. Mittar, S., Ulyatt, C., Howell, G. J., Bruns, A. F., Zachary, I., Walker, J. H. and Ponnambalam, S. 2009. VEGFR1 receptor tyrosine kinase localization to the Golgi apparatus is calcium-dependent. *Exp. Cell Res.* **315**: 877–889. [Medline] [CrossRef]

46. Mousavi, S. A., Skjeldal, F., Fønhus, M. S., Haugen, L. H., Eskild, W., Berg, T. and Bakke, O. 2019. Receptor-mediated endocytosis of VEGF-A in rat liver sinusoidal endothelial cells. *BioMed Res. Int.* **2019**: 5496197. [Medline] [CrossRef]

47. Olsson, A. K., Dimberg, A., Kreuger, J. and Claesson-Welsh, L. 2006. VEGF receptor signalling - in control of vascular function. *Nat. Rev. Mol. Cell Biol.* **7**: 359–371. [Medline] [CrossRef]

48. Park, J. E., Chen, H. H., Winer, J., Houck, K. A. and Ferrara, N. 1994. Placenta growth factor. Potentiation of vascular endothelial growth factor bioactivity, in vitro and in vivo, and high affinity binding to Flt-1 but not to Flk-1/KDR. *J. Biol. Chem.* **269**: 25646–25654. [Medline]

49. Rahimi, N. 2006. VEGFR-1 and VEGFR-2: two non-identical twins with a unique physiognomy. *Front. Biosci.* **11**: 818–829. [Medline] [CrossRef]

50. Rahimi, N., Dayanir, V. and Lashkari, K. 2000. Receptor chimeras indicate that the vascular endothelial growth factor receptor-1 (VEGFR-1) modulates mitogenic activity of VEGFR-2 in endothelial cells. *J. Biol. Chem.* **275**: 16986–16992. [Medline] [CrossRef]

51. Rebuzzi, L., Willmann, M., Sonneck, K., Gleixner, K. V., Florian, S., Kondo, R., Mayerhofer, M., Vales, A., Gruze, A., Pickl, W. F., Thalhammer, J. G. and Valent, P. 2007. Detection of vascular endothelial growth factor (VEGF) and VEGF receptors Flt-1 and KDR in canine mastocytoma cells. *Vet. Immunol. Immunopathol.* **115**: 320–333. [Medline] [CrossRef]

52. Roeckl, W., Hecht, D., Sztajer, H., Waltenberger, J., Yayon, A. and Weich, H. A. 1998. Differential binding characteristics and cellular inhibition by soluble VEGF receptors 1 and 2. *Exp. Cell Res.* **241**: 161–170. [Medline] [CrossRef]

53. Santos, S. C. and Dias, S. 2004. Internal and external autocrine VEGF/KDR loops regulate survival of subsets of acute leukemia through distinct signaling pathways. *Blood* **103**: 3883–3889. [Medline] [CrossRef]

54. Santos, S. C., Miguel, C., Domingues, I., Calado, A., Zhu, Z., Wu, Y. and Dias, S. 2007. VEGF and VEGFR-2 (KDR) internalization is required for endothelial recovery during wound healing. *Exp. Cell Res.* **313**: 1561–1574. [Medline] [CrossRef]

55. Stewart, M., Turley, H., Cook, N., Pezzella, F., Pillai, G., Ogilvie, D., Cartlidge, S., Paterson, D., Copley, C., Kendrew, J., Barnes, C., Harris, A. L. and Gatter, K. C. 2003. The angiogenic receptor KDR is widely distributed in human tissues and tumours and relocates intracellularly on phosphorylation. An immunohistochemical study. *Histopathology* **43**: 33–39. [Medline] [CrossRef]

56. Tas, J. 1977. The Alcian blue and combined Alcian blue—Safranin O staining of glycosaminoglycans studied in a model system and in mast cells. *Histochem. J.* **9**: 205–230. [Medline] [CrossRef]

57. Takahashi, H. and Shibuya, M. 2005. The vascular endothelial growth factor (VEGF)/VEGF receptor system and its role under physiological and pathological conditions. *Clin. Sci. (Lond.)* **109**: 227–241. [Medline] [CrossRef]

58. Vincent, L., Jin, D. K., Karajannis, M. A., Shido, K., Hooper, A. T., Rashbaum, W. K., Pytowski, B., Wu, Y., Hicklin, D. J., Zhu, Z., Bohlen, P., Niesvizky, R. and Rafii, S. 2005. Fetal stromal-dependent paracrine and intracrine vascular endothelial growth factor-a/vascular endothelial growth factor receptor-1 signaling promotes proliferation and motility of human primary myeloma cells. *Cancer Res.* **65**: 3185–3192. [Medline] [CrossRef]

59. Wang, Z., Mascarenhas, N., Eckmann, L., Miyamoto, Y., Sun, X., Kawakami, T. and Di Nardo, A. 2017. Skin microbiome promotes mast cell maturation by triggering stem cell factor production in keratinocytes. *J. Allergy Clin. Immunol.* **139**: 1205–1216.e6. [Medline] [CrossRef]

60. Waltenberger, J., Claesson-Welsh, L., Siegbahn, A., Shibuya, M. and Heldin, C. H. 1994. Different signal transduction properties of KDR and Flt1, two receptors for vascular endothelial growth factor. *J. Biol. Chem.* **269**: 26988–26995. [Medline]

61. Wilkes, L. K., McMenamin, C. and Holt, P. G. 1992. Postnatal maturation of mast cell subpopulations in the rat respiratory tract. *Immunology* **75**: 535–541. [Medline]

62. Yu, Y., Blokhuis, B. R., Garssen, J. and Redegeld, F. A. 2016. Non-IgE mediated mast cell activation. *Eur. J. Pharmacol.* **778**: 33–43. [Medline] [CrossRef]

63. Zhang, Y., Pillai, G., Gatter, K., Blázquez, C., Turley, H., Pezzella, F. and Watt, S. M. 2005. Expression and cellular localization of vascular endothelial growth factor A and its receptors in acute and chronic leukemias: an immunohistochemical study. *Hum. Pathol.* **36**: 797–805. [Medline] [CrossRef]

64. Zeng, H., Zhao, D. and Mukhopadhyay, D. 2002. Flt-1-mediated down-regulation of endothelial cell proliferation through pertussis toxin-sensitive G proteins, beta gamma subunits, small GTPase CDC42, and partly by Rac-1. *J. Biol. Chem.* **277**: 4003–4009. [Medline] [CrossRef]